



Numerical Modeling of Plasma Assisted Pyrolysis and Combustion of Ammonia

Taresh Sanjeev Taneja* and Suo Yang†

Department of Mechanical Engineering, University of Minnesota – Twin Cities, Minneapolis, MN 55455, USA

This work aims at studying the combustion and pyrolysis characteristics of ammonia (NH_3) using non-equilibrium plasma. The well known challenges of ammonia combustion and the advantages of using non-equilibrium plasma are discussed using results of zero-dimensional and one-dimensional coupled simulations. Periodic nanosecond pulsed discharges of plasma are interspersed with microsecond gaps of combustion to assess the assistance provided by plasma on overall combustion characteristics of ammonia fuel, such as ignition delay and flammability limit. Due to the lack of a reliable plasma mechanism for ammonia, a validated plasma kinetic mechanism of methane and oxygen is transformed to that of ammonia and oxygen, and is coupled with an experimentally validated ammonia combustion mechanism in this work. Another NH_3 / O_2 / He plasma mechanism that was recently assembled and published is also used to study the discharge and inter-pulse kinetics. A 0D model is developed to compute the rates of the electron impact reactions during the discharge, and ion-electron recombination reactions and quenching reactions along with the combustion reactions during the gap. Finally, the species concentrations and temperatures from this model are compared with those obtained using a detailed 1D model which solves for the transient electric field in addition to the species concentrations and temperature.

I. Nomenclature

e	= magnitude of charge of a single electron
E	= Electric field
N_{gas}	= Number density of neutral gas molecules
N_e	= Number density of electrons
h_i	= enthalpy of species i
t	= time
C_v	= Molar specific heat at constant volume
k_B	= Boltzmann Constant
T_{gas}	= Gas temperature
T_e	= Electron temperature
T_{wall}	= Wall temperature
L	= Electrode gap
W_i	= Molecular weight of species i
W_{mix}	= Average molecular weight of the mixture
Y_i	= Mass fraction of species i
V_{app}	= Applied Voltage
V_{gap}	= Gap Voltage
J	= Current Density
γ	= Specific heat ratio
ρ	= gas density
λ	= gas thermal conductivity
v_e	= electron drift velocity
H'_i	= enthalpy per molecule of species i
ω_i	= net production rate of species i

*Ph.D. Student, Student Member AIAA.

†Richard & Barbara Nelson Assistant Professor, suo-yang@umn.edu (Corresponding Author), Member AIAA.

II. Introduction

AMMONIA (NH_3) is often regarded as a renewable, carbon free alternative to conventional hydrocarbon based fuels. It is also considered as an H_2 -carrier fuel, which could make hydrogen combustion feasible for commercial applications. The advancement in renewable generation of ammonia using electrolysis of water to produce hydrogen and fractionation of air to produce nitrogen, and the improvements in the existing Haber-Bosch process of ammonia synthesis have affirmed much cleaner production of ammonia in the near future. Although, it is a common constituent of fertilizers, it has not successfully been used as a fuel despite its reasonable calorific value of 22.5 MJ/kg. The major limitations which have inhibited its adoption as an alternative, green fuel are its high heat of ignition, its narrow flammability range and excessive NO_x production. All these challenges can be addressed to a significant degree by aiding ammonia combustion with non-equilibrium plasma discharges. Furthermore, NH_3 is one of the primary contaminants in the commonly used Claus process used in the oil refining and gas processing industry to extract sulfur. Pyrolysis of ammonia is used to decompose it in the downstream reactors. Hence, applications such as these warrant the development of accurate kinetic mechanisms describing, both, the plasma and combustion chemistry. While there have been a few well validated combustion mechanisms in the literature, a well accepted plasma mechanism for NH_3 doesn't exist. However, as described in a recent publication [1], a plasma mechanism for ammonia has been assembled by taking reactions from multiple sources, which has also been tested in the present work using an in-house 0D plasma assisted combustion (PAC) solver.

Yang et al. [2] developed a 1D model for simulating combustion coupled with a periodic nanosecond dielectric barrier discharge. During the plasma pulse, the electron impact reactions are much faster in comparison to the other reactions, given their dependence on the reduced electric field (E/N). During the microsecond gaps after each pulse, electron-ion recombination reactions, de-excitation reactions and combustion chemistry reactions become predominant. As a result, species densities, gas and electron temperatures and the electric field are computed during the pulses whereas only the species densities and gas temperatures are computed between two pulses.

Lefkowitz et al. [3, 4] and Mao et al. [5, 6] described constant volume and constant pressure formulation based 0D models to simulate PAC of different fuel air mixtures which focus on different aspects such as the role of low temperature pathways and vibrationally excited species in the ignition enhancement of $\text{CH}_4/\text{O}_2/\text{He}$ mixtures, respectively. Both these models couple ZDPlasKin [7], a popular solver to model plasma kinetics, and CHEMKIN [8], a popular package to model combustion chemical kinetics. Moreover, ZDPlasKin interfaces with BOLSIG+ [9], a commonly used Boltzmann equation solver to compute the rate constants of electron impact reactions using the cross section data of the reactants. The present work describes the formulation of a similar 0D solver that is developed in-house, and a few details of the 1D solver that was tailored to simulate plasma assisted ammonia pyrolysis and combustion.

[1] provides an assembled NH_3 plasma mechanism and discusses the impact of pulse frequencies and pulse number on the ignition delay and the minimum initial temperature required to attain successful ignition with a given pulse input energy. Similar studies have also been conducted in [10], although for an H_2 -air system. The relative importance of thermal and kinetic effects on ignition enhancement due to a nanosecond discharge has also been discussed in this paper. Zhong et al. [11] investigated the kinetics of low temperature pathways for the pyrolysis and oxidation of n-dodecane/ O_2/N_2 mixtures using pulsed plasma discharge, with different experimental techniques. Using their model, they probed into the importance of N_2^* and the strong NO kinetic effects. Laser diagnostics and 1D numerical studies in [12] delineated the dominant pathways for the production of certain important derivatives of methane pyrolysis such as C_2H_2 and CH_2O . This work used the same 1D model as is described in the current paper.

III. Numerical Model

This section describes the plasma and combustion chemistry mechanisms for ammonia pyrolysis and combustion, and the governing equations and numerical schemes used in the 0D and 1D models.

A. Plasma and Combustion Kinetics Mechanism for NH_3

Due to the lack of an experimentally validated plasma mechanism for NH_3 pyrolysis and combustion, an experimentally validated $\text{CH}_4/\text{O}_2/\text{He}$ plasma mechanism [6] is converted to an $\text{NH}_3/\text{O}_2/\text{He}$ mechanism by simply replacing CH_4 with NH_3 , due to the molecular similarity. While this approach may not yield accurate results which can directly be used to investigate an actual NH_3 plasma discharge, it can nonetheless be considered a starting point, until an experimentally validated NH_3 plasma mechanism is developed. Another assembled plasma mechanism given in [1] is also tested with the 0D code. All C_xH_y species are transformed to N_xH_{y-1} species accordingly. The ionization, attachment,

effective and dissociative reactions from the Morgan [13] and Hayashi [14] databases on LXCat are also added, which are the only two, known cross section databases comprising of NH_3 electron impact reactions. The electronic and vibrational excitation reactions in these databases were skipped for the preliminary tests due to the lack of suitable relaxation reactions for these excited species. However, suitable electron - ion recombination reactions were constructed by transforming the CH_4 mechanism, for all the ionized species which would be generated during the pulse. Currently, the set of ionized species (resulting from direct NH_3 ionization) in the pyrolysis and combustion mechanisms in this research comprises of NH_3^+ , NH_3^- , NH_2^+ , NH^+ , NH_4^+ , N_2H_4^+ , N_2H_2^+ and H^+ only.

A detailed $\text{NH}_3/\text{O}_2/\text{N}_2$ combustion mechanism comprising of 38 species and 265 reactions, developed and validated by Mei et al. [15], is used in this research. A total of 55 species and 593 reactions were used in the plasma and combustion mechanisms together. A further subset of this mechanism consisting of reactions which involve only species containing the elements N and H exclusively, are used for plasma assisted pyrolysis simulations. The pyrolysis mechanism consists of 23 species and 88 reactions, including the plasma chemistry species and reactions. The CH_4 derived plasma mechanism consists of the vibrationally and electronically excited species of O_2 - $\text{O}_2(\text{v}1)$, $\text{O}_2(\text{v}2)$, $\text{O}_2(\text{v}3)$, $\text{O}_2(\text{A}1)$, $\text{O}_2(\text{B}1)$ and O_2^* in addition to the ionized NH_x species mentioned above. Moreover, the plasma mechanism assembled in [1] is also combined with the same [15] combustion mechanism to obtain more realistic results for the species densities and temperatures, as is discussed in the next section. However, this could only be used with the 0D solver, as the 1D simulation would take much longer to complete with a new mechanism. We plan to discuss the equivalence and interesting sheath layer phenomena with this new plasma mechanism, if any, in our subsequent articles.

B. Zero-Dimensional and One-Dimensional Coupled Model

A modeling strategy similar to [3] and [6] is followed in order to build a 0D plasma assisted combustion solver. Both constant volume and constant pressure reactor versions have been developed and validated with results published in the literature, and are shown in figures [1] 2a and 2b. Figures 2a and 2b show the validation of the current solver by comparing the species densities and ignition delay provided in [16] (a constant pressure case) and the temperature profile with that provided in [10] (a constant volume case). E/N and pulse duration are used as the only controlling parameters for energy deposition into the discharge. Since the zero-dimensional solver does not solve for the evolution of electric field, a high-enough constant value for E/N is chosen corresponding to the complete breakdown and ionization of the gas. Consequently, the pulse duration is set to 3 - 4 ns, which is much smaller as compared to practical nanosecond pulses which typically last for 30 - 80 ns. The E/N value and the pulse energy are adjusted in order to match the temperature and species concentrations obtained from the 1D solver, which accounts for the sheath layer formation near the electrodes.

Governing equations for species concentration evolution which are solved during the pulse are described in [7]. Equation (3) constitutes the source term, P_{gas} of the energy equation. The constant pressure version of the equation is given in equation (2)

$$\frac{dN_i}{dt} = \sum_{j=1}^{j_{\text{max}}} Q_{ij}(t) \quad (1)$$

$$\frac{\gamma}{\gamma - 1} \frac{d(N_{\text{gas}} T_{\text{gas}})}{dt} = P_{\text{gas}} \quad (2)$$

$$P_{\text{gas}} = P_{\text{ext}} - P_{\text{chem}} - P_{\text{elec}} \quad (3)$$

$$P_{\text{ext}} = e N_e E v_e \quad (4)$$

$$P_{\text{chem}} = \sum_{i=1}^{i_{\text{max}}} H'_i \frac{dN_i}{dt} \quad (5)$$

$$P_{\text{elec}} = \frac{3}{2} k_B \frac{d(N_e T_e)}{dt} \quad (6)$$

The lumped energy source term approach is used in this version of the 0D code, where the energy equation (2) is not explicitly solved during the pulse; instead the source term given in equation (3) is used to update the temperature at the end of each pulse. This update is done using Newton iteration, by incrementing the datum of the overall enthalpy

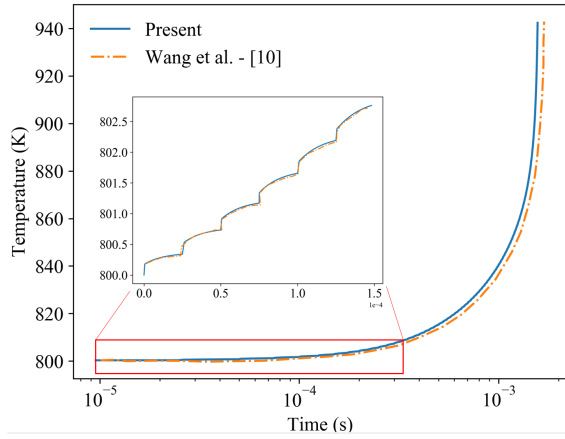


Fig. 1 Temperature Comparison with [10]

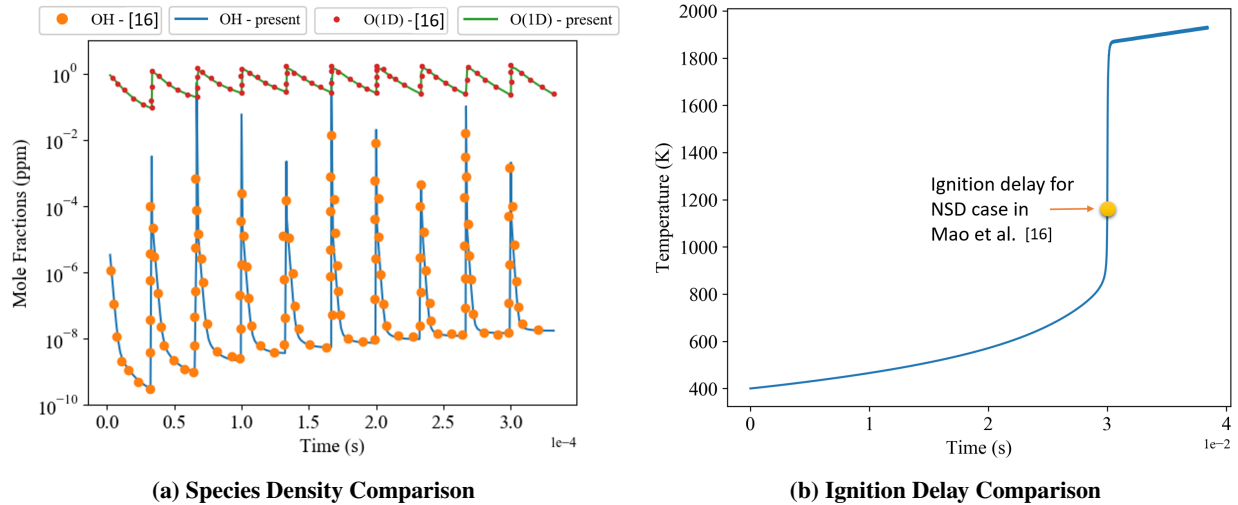


Fig. 2 Validation of 0D Solver with [16]

(internal energy for the constant volume case) with the lumped energy source term, P_{gas} of the previous pulse. Following which, the Newton iteration method is used to update the temperature, based on the evolution of the species mass fractions at each time step, instead of using a temporal finite difference approximation, such as the first order Euler method.

The electron impact reactions, along with the other plasma reactions are solved using ZDPlasKin throughout the entire duration. Combustion / pyrolysis chemistry is assumed to be "frozen" during the pulses. The species concentration and temperature equations are given in (7) and (8), which are eventually solved using CHEMKIN-III subroutines. The optional conduction heat loss term, with an equivalent gap length scale of L/π is also included to account for reactor wall heat losses as suggested by Adamovich et al. [17]. DVODE [18] is used for implicit time integration of the coupled ODEs.

$$\frac{dY_i}{dt} = \frac{\omega_i W_i}{\rho} \quad (7)$$

$$\frac{dT_{gas}}{dt} = \frac{-1}{\rho C_p} \left[\sum_{i=1}^{i_{max}} h_i \omega_i W_i + W_{mix} \lambda(T_{gas}) \frac{T_{gas} - T_{wall}}{(L/\pi)^2} \right] \quad (8)$$

The equations solved in the parallel 1D solver can be found in [2]. Unlike the 0D model, this model solves for the spatially varying electric potential at each time step with the updated charged species densities based source term.

Convection and diffusion fluxes of species densities, electron density and electron energy density are computed at each time step. The 1D solver uses adaptive multi-time scale time-steps, based on the convection time scale, electron energy relaxation time scale and the dielectric relaxation time scale. These typically range from 2×10^{-13} s during the breakdown, to around 4×10^{-12} s during the end of the discharge. The time-step is then ramped up to 1 ns during the gap, when the electric field (and thus the Poisson equation solver) is turned off. These extremely small time-steps render the 1D code to be quite slow, even though it uses domain parallelism. The 0D solver, on the other hand, uses a time-step of 5×10^{-11} s during the discharge, and around 5 ns, during the gaps. While the temperatures and species densities remain fairly uniform in the central core region of the 1D domain, the dominant plasma sheath formation is evident from the species densities plots shown in the next section.

IV. Results and Discussion

A. Comparison of 0D and 1D results for Ammonia pyrolysis and combustion

The 1D solver and the 0D solver were both used to simulate ammonia pyrolysis and combustion using the mechanisms described above. The species densities of certain important species, obtained using both the codes are plotted in figures 4 and 5. The densities at the mid-point of the 1D domain are compared with the densities obtained from the 0D simulations. The pulse width in the 1D code, was set to 35 ns and 60 ns for the pyrolysis and combustion simulations, respectively. The frequency of the pulses was set to 30 kHz for both the cases. A Gaussian, time varying profile was used to fit typical experimental nanosecond discharge voltages for both the cases, in the 1D code. The resulting gap voltage and electric field were solved using equation 2 in [2]. The 0D solver uses a square wave profile for E/N, with a much shorter pulse duration of 5 - 9 ns. A constant value of 100 Td was set for the reduced electric field in these simulations. Moreover, an initial temperature of 300 K and a constant pressure of 60 Torr was used in both the simulations. An equivalence ratio of 1.15 was used for this comparison.

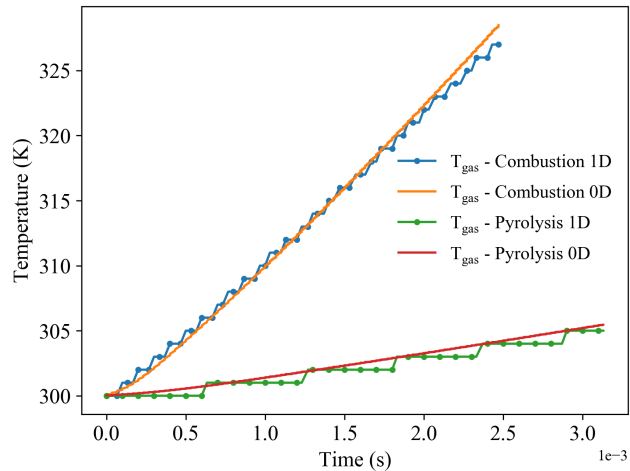


Fig. 3 Gas Temperature: 0D vs 1D

It was found that the E/N value didn't affect the simulation results of this weakly-ionized plasma by much (temperature and densities were within a 5% range), as long as it was between 100 - 200 Td. The pulse width varied with each pulse, depending on the electron number density, and the degree of ionization, to ensure constant input energy deposition per pulse. The external input energy per pulse, per unit volume, was used as one of the free parameters in the 0D simulation. This method is described in [16]. For the present results, temperature was used as the only target to adjust the pulse energy in the 0D solver, which was set to 0.0075 mJ/cm^3 for the pyrolysis case and 0.025 mJ/cm^3 for the combustion case. The temperature comparison, which is used as a reference, is shown in figure 3. In this work, only 95 pulses for the pyrolysis case and 75 pulses for the combustion case were simulated, given the slow speed of the 1D solver.

As is shown in figure 4, a reasonable agreement (within one order of magnitude) was observed between the 0D and 1D results for the species densities of NNH, NH_4^+ , NH_2 and H radical in the pyrolysis case. Good agreement was observed in 5 for species which participate in both the plasma and combustion mechanism reactions, such as NO_2 , NO and OH, whereas discrepancies were observed in the excited and ionized species, such as O(1D), $\text{O}_2(\text{v}2)$, and NH_4^+ ,

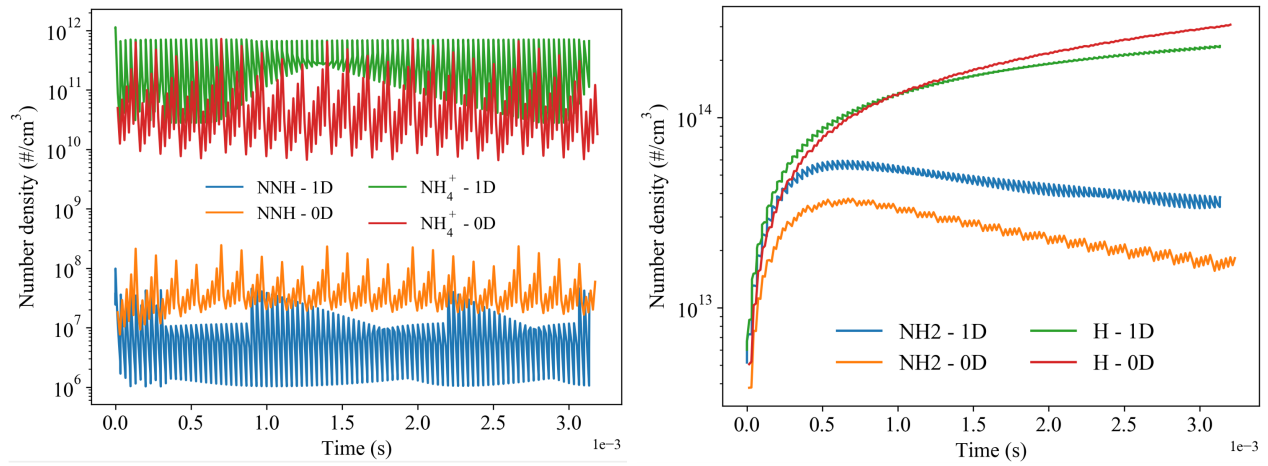


Fig. 4 0D vs 1D Pyrolysis - Species Density Comparison

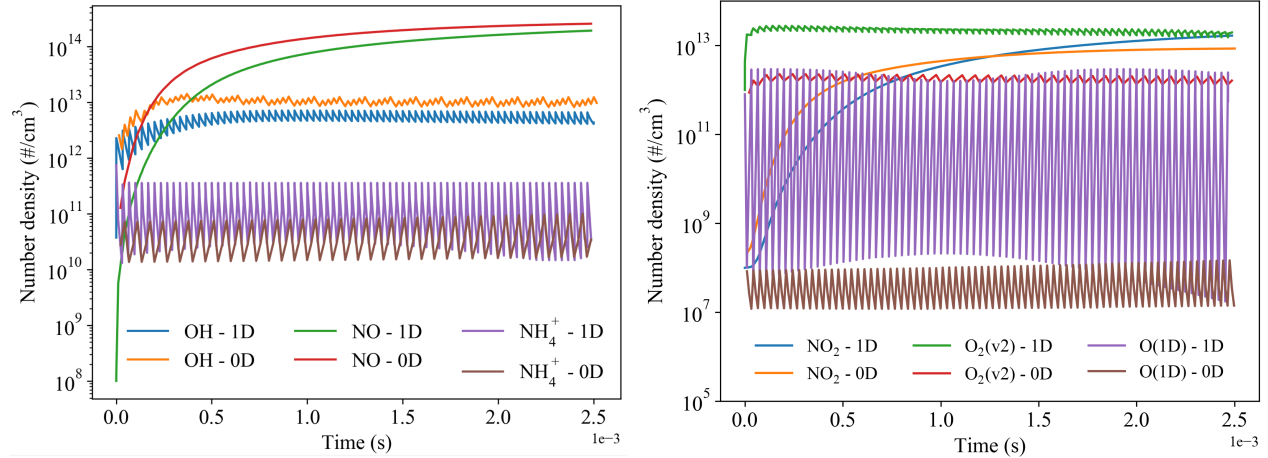


Fig. 5 0D vs 1D Combustion - Species Density Comparison

which are only "active" during the discharge. These are some of the important species listed in [1]. A detailed path flux analysis is essential to determine the cause of the minor discrepancies in these results, however, one can attribute these differences mainly to a combination of species diffusion effect and spatially varying electric fields in the 1D simulation, which are absent in the 0D simulation. The particularly sensitive case of O(1D) measurements are also discussed in [19], where the importance of this radical in the chain branching reactions with unsaturated hydrocarbon mixtures is discussed in detail. Furthermore, the 1D solver uses fitting coefficients of a 5-term exponential variation for computing the reaction rates of the electron impact reactions, which are obtained from BOLSIG+. This is mainly done to speed-up the already slow 1D solver and to make it more robust. Although, this comes at the cost of accuracy in some cases. The 0D solver directly interfaces with the BOLSIG library, and thus the rate coefficients can be assumed to be accurate, thereby leaving only the uncertainty associated with the cross section database measurements as the only potential source of error - which is a common input for both the solvers.

Finally, figure 6 shows the spatial variation of some charged and excited species, including electrons, at the end of the 75th pulse (2.5 ms) for the combustion case. The plasma sheath layer formation is evident from the peaks in the species densities in these plots, which is attributed to the much higher E/N value near the electrodes, which in turn leads to faster reaction rates of the plasma reactions. Fundamentally, this occurs due to the much higher electron mobility, because of its low mass and high velocity, as compared to the other ions. Consequently, the electrons drift from the central uniform plasma region towards the electrode walls, and a region of positively charged species forms around the electrons.

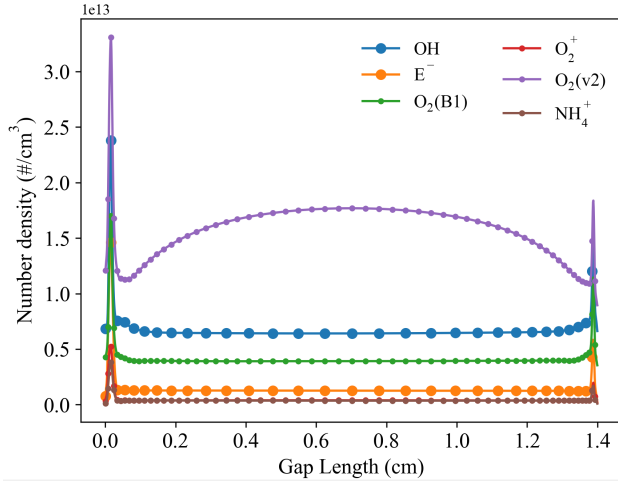


Fig. 6 Gas Temperature: 0D vs 1D

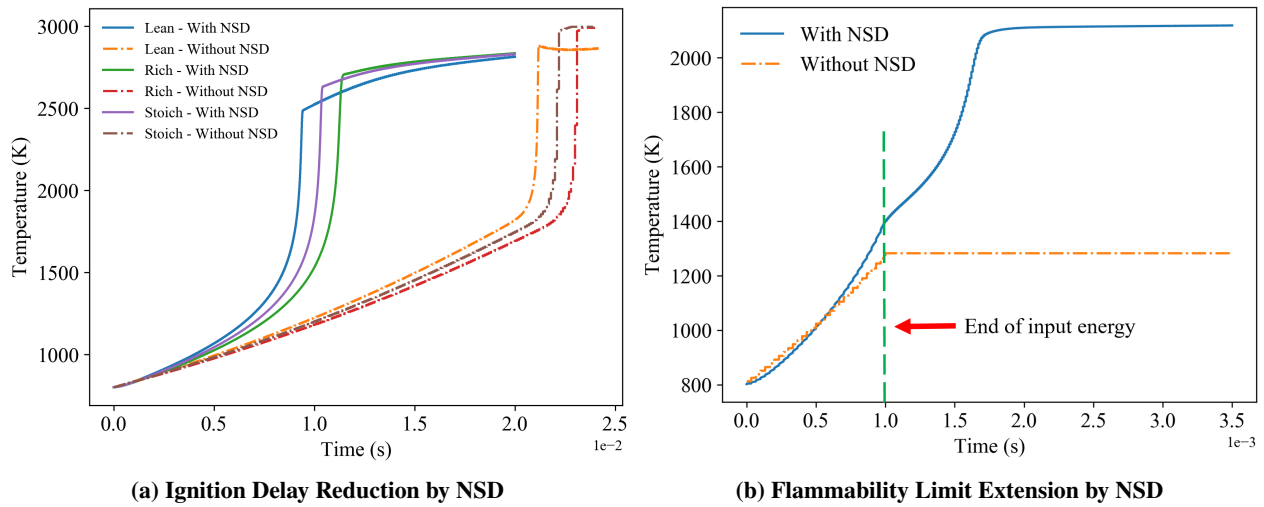
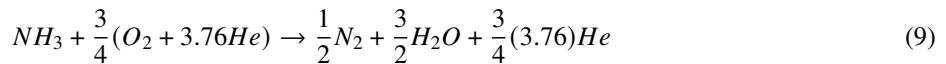


Fig. 7 Effect of Nanosecond Discharge on Ignition Characteristics of NH_3

B. Effect of plasma discharge on ignition delay and flammability limits of NH_3 combustion

Using the plasma mechanism listed in [11], and the experimentally validated combustion mechanism in [15], 0D simulations are done to test the efficacy of nanosecond discharges on overall combustion for 3 different equivalence ratios. The global reaction used to calculate the equivalence ratio is given in (9). Here, helium is used as a substitute for nitrogen in air. Thus, the molar ratio of He: O_2 is maintained as 3.76:1.



Cases with lean ($\phi = 0.75$), stoichiometric ($\phi = 1.0$), and rich ($\phi = 1.25$) mixtures are simulated using the 0D solver. The initial temperature and pressure are maintained at 800 K and 60 Torr, respectively. A constant E/N with variable pulse width, but constant input energy of 0.04 mJ/cm³ is used in the simulation. To compare the ignition delay enhancement due to the NSD, similar cases with the same input energy per pulse (now viewed as thermal energy input), but with no electric field are analyzed in figure 7a.

The total input energy is, in fact, much greater for the cases without NSD, as those mixtures are heated with the same input energy, at the same frequency until they ignite - which happens much later as compared to the cases with NSD. The ignition delays for the cases with NSD are 8.1 ms (lean), 10.2 ms (stoichiometric) and 11.1 ms (rich). The corresponding ignition delays for cases without plasma are 21.0 ms (lean), 22.3 ms (stoichiometric) and 23.4 ms (rich).

Finally, the lean flammability limit was tested for a very lean equivalence ratio of 0.4. While practically this mixture might not be combustible, in a homogeneous constant pressure premixed reactor, non-equilibrium plasma can ignite such a mixture successfully. This is tested by supplying 0.4 mJ/cm³/pulse, of constant input power for 30 pulses, with a frequency of 30 kHz, in the first case. This energy is in the form of a pulsed discharge, with a reduced electric field of 140 Td. In the second case, the same input energy is supplied in the form of thermal energy (E/N = 0), at the same frequency, for the same total duration. Thus, the total energy and the frequency remain same for both cases. Figure 7b shows successful ignition for the first case only, despite the removal of electrical energy after 30 pulses. This happens due to the radical pool that is developed by the plasma discharge, which effectively extends the flammability limit of the mixture. On the other hand, thermal ignition (without NSD) can not ignite such a lean mixture.

V. Conclusion and Future Work

Two pairs of plasma chemistry mechanisms were used along with a validated combustion mechanism to simulate nanosecond discharge of plasma assisted pyrolysis and combustion of ammonia. A 0D PAC solver was developed and the results were compared with a 1D PAC solver. The 0D solver was validated with results from the literature with two different papers. The efficacy of plasma in reducing the ignition delay was tested with lean, stoichiometric and rich mixtures of ammonia with oxygen and helium. Extension of the lean flammability limit of ammonia was tested up to an equivalence ratio of 0.4. Furthermore, sheath layer effects were observed in the 1D simulation of the mixture between two parallel plate electrodes. While the species densities remained mostly uniform in the central region of the 1D domain, species diffusion effects and the spatial variation of electric field could have caused the differences in species densities.

It is imperative to test the 1D solver results for cases with successful ignition to understand the impact of sheath layer dynamics on the flammability limit and ignition delays. Certainly, this needs to be done with high fidelity plasma mechanisms, for which 1D could be one candidate, provided there is experimental validation in the near future. Moreover, reasons for discrepancies in the 1D and 0D models in predicting the species densities need to be probed into, to find ways to make the 0D solver predictions more "realistic". Detailed path flux analysis at several points in the 1D domain could provide significant insight into the exact reasons. Similar studies will also be carried out at higher pressures, and the impact of the pressure dependent reactions will be discussed. With the end goal of building a simulation tool that can simulate turbulent PAC, the 1D solver is a step in the right direction as it provides insight into the sheath layer kinetics which may be important to determine the wall heat loss at the electrode surface and the subsequent minimum ignition energy in practical DBD combustors. However, using detailed chemistry will be too prohibitive to work with, given the extreme limitations on time-step, with increase in dimensionality.

Acknowledgments

S. Yang gratefully acknowledges the faculty start-up funding from the University of Minnesota. T. Taneja acknowledges the fruitful discussions with Dr. Xingqian Mao, Dr. Yuan Wang, Mr. Timothy Chen and Ms. Galia Faingold during the development of the 0D solver and for choosing the correct plasma mechanism for ammonia. Both authors gratefully acknowledge Prof. Graham V. Candler and the Minnesota Supercomputing Institute (MSI) for the computational resources.

References

- [1] Faingold, G., and Lefkowitz, J. K., "A numerical investigation of NH₃/O₂/He ignition limits in a non-thermal plasma," *Proceedings of the Combustion Institute*, 2020.
- [2] Yang, S., Nagaraja, S., Sun, W., and Yang, V., "Multiscale modeling and general theory of non-equilibrium plasma-assisted ignition and combustion," *Journal of Physics D: Applied Physics*, Vol. 50, No. 43, 2017, p. 433001. <https://doi.org/10.1088/1361-6463/aa87ee>
- [3] Lefkowitz, J. K., Guo, P., Rousso, A., and Ju, Y., "Species and temperature measurements of methane oxidation in a nanosecond repetitively pulsed discharge," *Philosophical Transactions of the Royal Society A: Mathematical, Physical and Engineering Sciences*, Vol. 373, No. 2048, 2015, p. 20140333. <https://doi.org/10.1098/rsta.2014.0333>
- [4] Lefkowitz, J. K., Guo, P., Rousso, A., and Ju, Y., "Low temperature oxidation of methane in a nanosecond pulsed plasma discharge," *53rd AIAA Aerospace Sciences Meeting*, 2015, p. 0665.

- [5] Mao, X., Rousso, A. C., Chen, Q., and Ju, Y., "Modeling of ignition enhancement of CH₄/O₂ mixtures by non-equilibrium excitation of reactants using hybrid nanosecond-pulsed discharge and DC discharge," *2018 AIAA Aerospace Sciences Meeting*, 2018, p. 0928.
- [6] Mao, X., Rousso, A., Chen, Q., and Ju, Y., "Numerical modeling of ignition enhancement of CH₄/O₂/He mixtures using a hybrid repetitive nanosecond and DC discharge," *Proceedings of the Combustion Institute*, Vol. 37, No. 4, 2019, pp. 5545–5552.
- [7] Pancheshnyi, S., Eismann, B., Hagelaar, G., and Pitchford, L., "Computer code ZDPlasKin, University of Toulouse, LAPLACE," Tech. rep., CNRS-UPS-INP, Toulouse, France www.zdplaskin.laplace.univ-tlse.fr, 2008.
- [8] Kee, R., Rupley, F., Miller, J., Coltrin, M., Grcar, J., Meeks, E., Moffat, H., Lutz, A., Dixon-Lewis, G., Smooke, M., et al., "CHEMKIN Collection, Release 3.6, Reaction Design," *Inc., San Diego, CA*, Vol. 20, No. 0, 2000, p. 0.
- [9] Hagelaar, G., and Pitchford, L., "Solving the Boltzmann equation to obtain electron transport coefficients and rate coefficients for fluid models," *Plasma Sources Science and Technology*, Vol. 14, No. 4, 2005, p. 722.
- [10] Guo, P., Chen, H., Chen, Z., et al., "Numerical modeling of ignition enhancement by repetitive nanosecond discharge in a hydrogen/air mixture—Part I: Calculations assuming homogeneous ignition," *Journal of Physics D: Applied Physics*, 2020.
- [11] Zhong, H., Mao, X., Rousso, A. C., Patrick, C. L., Yan, C., Xu, W., Chen, Q., Wysocki, G., and Ju, Y., "Kinetic study of plasma-assisted n-dodecane/O₂/N₂ pyrolysis and oxidation in a nanosecond-pulsed discharge," *Proceedings of the Combustion Institute*, 2020.
- [12] Chen, T. Y., Taneja, T. S., Rousso, A. C., Yang, S., Kolemen, E., and Ju, Y., "Time-resolved in situ measurements and predictions of plasma-assisted methane reforming in a nanosecond-pulsed discharge," *Proceedings of the Combustion Institute*, 2020.
- [13] "Morgan Database," www.lxcat.net, 1987.
- [14] "Hayashi Database," www.lxcat.net, 1987.
- [15] Mei, B., Zhang, X., Ma, S., Cui, M., Guo, H., Cao, Z., and Li, Y., "Experimental and kinetic modeling investigation on the laminar flame propagation of ammonia under oxygen enrichment and elevated pressure conditions," *Combustion and Flame*, Vol. 210, 2019, pp. 236–246.
- [16] Mao, X., Chen, Q., Rousso, A. C., Chen, T. Y., and Ju, Y., "Effects of controlled non-equilibrium excitation on H₂/O₂/He ignition using a hybrid repetitive nanosecond and DC discharge," *Combustion and Flame*, Vol. 206, 2019, pp. 522–535.
- [17] Adamovich, I. V., Nishihara, M., Choi, I., Uddi, M., and Lempert, W. R., "Energy coupling to the plasma in repetitive nanosecond pulse discharges," *Physics of Plasmas*, Vol. 16, No. 11, 2009, p. 113505.
- [18] Brown, P., Hindmarch, A., and Byrne, G., "Dvode," *Computer Subroutine Package for Solving Ordinary Differential Equations*, (August 31, 1992), 1992.
- [19] Yan, C., Teng, C. C., Chen, T., Zhong, H., Rousso, A., Zhao, H., Ma, G., Wysocki, G., and Ju, Y., "The kinetic study of excited singlet oxygen atom O (1D) reactions with acetylene," *Combustion and Flame*, Vol. 212, 2020, pp. 135–141.